Journal of Molecular Structure 1042 (2013) 37–44

Contents lists available at SciVerse ScienceDirect

Journal of Molecular Structure

journal homepage: www.elsevier.com/locate/molstruc

Vibrational and conformational analysis on-N^1-N^2-bis((pyridine-4-yl)methylene) benzene-1,2-diamine

S. Subashchandrabose [a], C. Meganathan [b], Y. Erdoğdu [c], H. Saleem [d,*], C. Jajkumar [e], P. Latha [e]

[a] Dept. of Physics, M.A.R. College of Engineering & Technology, Trichy, Tamil Nadu 621 316, India
[b] Dept. of Physics, G.K.M. College of Engineering & Technology, Perungalathur, chennai, Tamil Nadu 600 063, India
[c] Dept. of Physics, Ahi Evran University, Kirsehir 40040, Turkey
[d] Dept. of Physics, Annamalai University, Annamalai Nagar, Tamil Nadu 608 002, India
[e] Dept. of Chemistry, FEAT Annamalai University, Annamalai Nagar, Tamil Nadu 608 002, India

HIGHLIGHTS

- Structural properties of NBPMB.
- TED.
- NBO analysis.
- NLO.
- Band gap energy.

ARTICLE INFO

Article history:
Received 16 December 2012
Received in revised form 17 March 2013
Accepted 17 March 2013
Available online 26 March 2013

Keywords:
FT-IR
FT-Raman
TED
NBO
Hyperpolarizability
HOMO–LUMO

ABSTRACT

The molecule N^1-N^2-bis((pyridine-4-yl)methylene)benzene-1,2-diamine (NBPMB) was synthesized and characterized by FT-IR, FT-Raman and UV–Vis., spectra. To identify the stable structure of the molecule meticulous conformational analysis was performed. The observed (FT-IR and FT-Raman) spectral frequencies were compared with harmonic wavenumbers. The vibrational assignments were performed on the basis of the total energy distribution (TED). The optimized geometrical parameters are calculated and compared with experimental results. The non-linear optical behavior NBPMB molecule is analyzed using hyperpolarizability calculation. The charge transfer within the molecule and biological activity of NBPMB were calculated.

1. Introduction

Schiff base which contain an azomethane group attracts much interest in synthetic chemistry. Some donor atoms such as N, O, S in Schiff bases have structural similarities with natural biological systems and imports in elucidating the mechanism of transformations and racemisation reactions due to presence of imine (—N═CH—) group [1]. It is also known to have biological activities such as antibacterial [2,3], antifungal [4,5], antitumor [6,7], antioxidant [8] and anti-tuberculosis [9] activities. In organic molecules the presence of —N═C— along with other functional groups form more stable complexes compared to compounds with only —N═C— coordinating moiety. Amino pyridine is a non-linear optical material, which were of great interest with good susceptibilities have their application in the field of photonics and also many areas in chemistry. 4-*N*,N^1-Dimethylaminopyridine has been become one of the most popular catalyst for different process such as acylations, alkylations, silylations, Baylis–Hilman reaction and nucleophillic substitutions of alcohols and amines [10]. The vibrational spectra of substituted pyridine have been the subject of several investigations [11–14].

Pyridine is also called azabenzene and azine, is a heterocyclic aromatic tertiary amine characterized by a six membered ring structure composed of five carbon atoms and one carbon–hydrogen atom in the benzene ring being replaced by a nitrogen atom. Pyridine and its related derivatives were found in the structure of many drugs. It has been extensively studied from the spectroscopic point of view, due in part to its presence in many chemical structures of high interest in a variety of biomedical and industrial fields. To the best of our

* Corresponding author. Tel.: +91 9443879295.
E-mail addresses: saleem_h2001@yahoo.com, sscbphysics@gmail.com (H. Saleem).

0022-2860/$ - see front matter © 2013 Elsevier B.V. All rights reserved.
http://dx.doi.org/10.1016/j.molstruc.2013.03.034

knowledge neither quantum chemical calculations nor the vibrational spectra of N^1-N^2-bis((pyridine-4-yl)methylene)benzene-1,2-diamine (NBPMB) have been reported so for. Therefore, the present investigation was undertaken to study the vibrational spectra of this molecule and to identify the various modes with greater wavenumber accuracy. In recent years, DFT calculations have been used extensively for calculating a wide variety of molecular properties such as equilibrium structure, charge distribution, FT-IR, NMR spectra and provided reliable results which are in agreement with experimental data [15]. In this research, Beck's three-parameter exchange functional [16] with Lee, Yang and Parr's [17] correlation functional (B3LYP) were used to perform the theoretical calculations such as harmonic wavenumber, molecular polarizability, NBO analysis, thermodynamic properties and few quantum descriptors of the title compounds.

2. Experimental details

2.1. Synthesis

An ethanolic solution of o-phenylenediamine was refluxed with 4-pyridine carboxaldehyde [1:2 ratios] for about 5 to 6 h. The volume of the solution was reduced to one third. The pale yellow solid formed after 1 day and precipitation was filtered and then recrystallized from ethanol.

2.2. FT-IR and FT-Raman spectra

The FT-IR spectrum of NBPMB was recorded in the region 400–4000 cm^{-1} on an IFS 66 V spectrophotometer using the KBr pellet technique. The spectrum was recorded at room temperature with a scanning speed of 10 cm^{-1} per minute and at the spectral resolution of 2.0 cm^{-1} in CISL Laboratory, Annamalai University, Tamilnadu, India. The FT-Raman spectrum of title compound was recorded using the 1064 nm line of a Nd:YAG laser as excitation wavelength in the region 50–3500 cm^{-1} on Bruker model IFS 66V spectrophotometer equipped with an FRA 106 FT-Raman module accessory and at spectral resolution of 4 cm^{-1}. The FT-Raman spectral measurements were carried out from Sree Chitra Tirunal, Institute of Medical Sciences and Technology, Poojappura, Thiruvananthapuram, Kerala, India.

3. Computational details

In order to establish the stable possible conformations, the conformational space of NBPMB was scanned with molecular mechanic simulations. This calculation was performed with the Spartan 08 program [18]. For meeting the requirements of both accuracy and computing economy, theoretical methods and basis sets were considered. DFT has been proved to be extremely useful in treating electronic structure of molecules. The entire calculations were performed at DFT level on a Pentium IV/3.02 G.Hz personal computer using Gaussian 03 W [19] program package, invoking gradient geometry optimization [19,20]. In this study, the conformer one is used for the geometry optimization. Initial geometry generated from standard geometrical parameters was minimized without any constraint in the potential energy surface at DFT level, adopting the standard 6-31G(d,p) basis set. The optimized structural parameters were used in the vibrational frequency calculations at the DFT level to characterize all stationary points as minima. Then vibrationaly averaged nuclear positions of NBPMB were used for harmonic vibrational frequency calculations resulting in IR and Raman frequencies together with intensities and Raman depolarization ratios. The vibrational modes were assigned on the basis of TED analysis using SQM program [21].

It should be noted that Gaussian 03 W package was able to calculate the Raman activity. The Raman activities were transformed into Raman intensities using Raint program [22] by the expression:

$$I_i = 10^{-12} \times (v_0 - v_i)^4 \times \frac{1}{v_i} \times RA_i \quad (1)$$

where I_i is the Raman intensity, RA_i is the Raman scattering activities, v_i is the wavenumber of the normal modes and v_0 denotes the wavenumber of the excitation laser [23].

4. Results and discussion

4.1. Conformational stability

To find the stable conformers, a meticulous conformational analysis was carried out for the NBPMB compound. Rotating 360 degree with intervals of 10° around the free rotation bonds, conformational space of the title compound was scanned by molecular mechanic simulations and then full geometry optimizations of these structures were performed by B3LYP/6-31G(d,p) method. Results of geometry optimizations were indicated that the title compound may have at least three conformers as shown in Fig. S1 (Supporting information). Ground state energies, zero point corrected energies (Eelect.+ZPE), relative energies and dipole moments of conformers were presented in Table S1 (Supporting information). The conformer one is the most stable one and the theoretical geometry of the title compound fairly well reproduce the experimental one [24,25]. The results and discussion of this paper is based on conformer one.

4.2. Molecular geometry

The optimized molecular geometry of NBPMB were calculated by using DFT/B3LYP/6-31G(d,p) basis set which is given in Table S2 (Supporting information). The numbering scheme of the molecule is given in Fig. 1. The exact crystal structure of the title compound is not yet discovered so that the optimized structure can only be compared with other similar system, e.g. 2, 6-bis [3-methoxysalicylidene)hydrazinocarbonyl] pyridine [25] and 5-(phenylazo)-N-(2-amino pyridine) salicylidene [24]. It is evident from Table S2, the optimized bond lengths and bond angles were

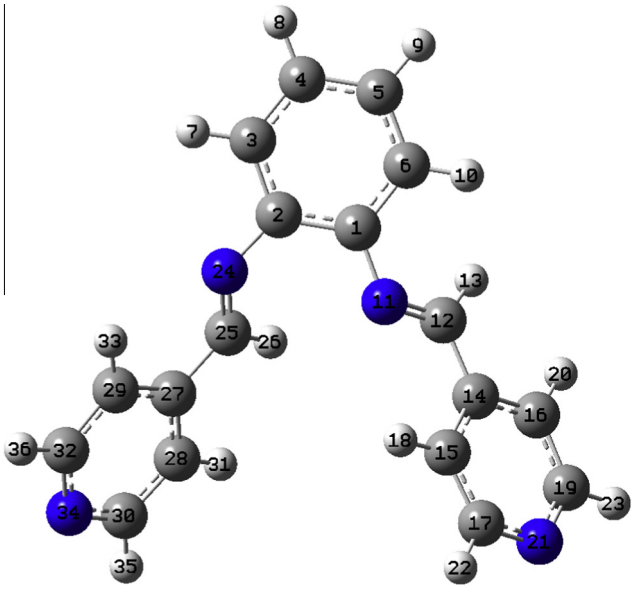

Fig. 1. The optimized molecular structure of NBPMB.

Table 1
Vibrational wave numbers obtained for NBPMB at B3LYP/6-31G(d,p) [harmonic frequency (cm^{-1}), IR , Raman intensities (km/mol), reduced masses (amu) and force constants ($mdynA^{\circ-1}$)].

Mode nos.	Calculated frequencies (cm^{-1})		Observed frequencies (cm^{-1})		Intensities		Vibrational assignments TED[d] ($\geqslant$10%)
	Unscaled	Scaled[a]	FT-IR	FT-Raman	I_{IR}[b]	I_{Raman}[c]	
1	25	24			0.03	33.62	$\delta_{CCN}(31) + \delta_{CNC}(16)$
2	27	25			0.30	1.91	$\Gamma_{C12N11C1C2}(17) + \Gamma_{C12N11C1C6}(12) + \Gamma_{C25N24C2C1}(18) + \Gamma_{C25N24C2C3}(12)$
3	32	30			0.31	84.82	$\Gamma_{CNCC}(22) + \Gamma_{CCCH}(15) + \Gamma_{CCCN}(10)$
4	61	58			0.02	20.69	$\delta_{CNC}(21) + \Gamma_{CNCC}(15) + \Gamma_{CCCN}(12)$
5	64	61			0.06	0.22	$\Gamma_{C14C12N11C1}(18) + \Gamma_{C27C25N24C2}(18)$
6	78	75			0.23	6.84	$\delta_{C12N11C1}(14) + \delta_{C25N24C2}(14)$
7	117	113		116s	3.79	38.35	$\Gamma_{C12N11C1C2}(11) + \Gamma_{C25N24C2C1}(11)$
8	133	128			8.88	18.68	$\Gamma_{C12N11C1C2}(11) + \Gamma_{C25N24C2C1}(11)$
9	157	151			2.74	2.07	$\delta_{CCC}(30) + \Gamma_{CCNC}(10)$
10	173	166			0.01	0.17	$\delta_{CCN}(18) + \delta_{CCC}(18)$
11	236	227			0.00	4.28	$\delta_{C12N11C1}(13) + \delta_{C25N24C2}(13)$
12	258	248			0.86	10.90	$\Gamma_{CCCC}(23) + \Gamma_{CCCN}(16)$
13	268	258			3.84	28.25	$\Gamma_{CNCC}(18)$
14	304	292			0.42	0.40	$\delta_{CCC}(14) + \Gamma_{CCCN}(10)$
15	308	296			0.16	2.82	$\Gamma_{CCNC}(14) + \delta_{CCC}(30)$
16	384	369			3.18	0.12	$\delta_{CCC}(24) + \Gamma_{CCCC}(20)$
17	390	375			0.01	0.09	$\Gamma_{N21C17C15C14}(10) + \Gamma_{N34C32C29C27}(10)$
18	391	375			0.03	0.36	$\Gamma_{N21C17C15C14}(10) + \Gamma_{N34C32C29C27}(10)$
19	455	437	426w		4.34	0.15	$\delta_{CCN}(16) + \delta_{CCC}(16)$
20	476	457	465w		6.20	7.05	$\delta_{CCN}(12) + \Gamma_{CCCC}(16)$
21	515	495	499w		25.04	1.94	$\delta_{CCC}(28)$
22	531	511			2.34	0.42	$\Gamma_{CNCC}(16)$
23	550	529	537w		17.80	1.75	$\Gamma_{CCNC}(11)$
24	572	550			10.83	0.33	$\delta_{CCC}(24)$
25	583	560	564w		4.09	2.64	$\Gamma_{C6C5C4C3}(15)$
26	583	561			1.72	0.84	$\delta_{C2C1N11}(12) + \delta_{N24C2C1}(12)$
27	645	620	618w		10.30	2.63	$\delta_{C4C3C2}(10) + \delta_{C1C6C5}(10) + \delta_{CNC}(12)$
28	677	650		652w	4.11	0.07	$\delta_{CNC}(24) + \delta_{CCN}(10)$
29	683	656			0.41	1.58	$\delta_{CCC}(28) + \delta_{NCC}(32)$
30	683	657	670w		0.49	1.22	$\delta_{CCC}(27) + \delta_{NCC}(31)$
31	745	716	712 ms		0.06	0.20	$\Gamma_{CCCC}(26) + \Gamma_{CNCC}(16)$
32	755	725			2.73	0.05	$\Gamma_{CCCC}(16) + \Gamma_{NCCC}(20)$
33	765	735			0.06	0.07	$\Gamma_{CCCC}(13)$
34	770	740	743 ms		39.10	1.55	$\Gamma_{H8C4C3C2}(14) + \Gamma_{C6C5C4H8}(12) + \Gamma_{H9C5C4C3}(12) + \Gamma_{C1C6C5H9}(14)$
35	821	789	768 ms		13.76	1.50	$\nu_{C2C1}(37) + \nu_{CC}(28) + \nu_{NC}(14)$
36	836	803			31.03	0.17	$\Gamma_{HCCC}(56) + \Gamma_{NCCH}(18)$
37	837	805	812w		4.70	0.09	$\Gamma_{HCCC}(52)$
38	867	833	823w		5.88	0.98	$\Gamma_{HCCC}(22) + \Gamma_{CCCH}(12)$
39	869	835			7.20	1.07	$\delta_{C5C4C3}(12) + \delta_{C6C5C4}(12)$
40	893	858	851w		3.35	6.73	$\nu_{CC}(24) + \delta_{CNC}(10) + \delta_{CCN}(12)$
41	898	862			0.74	0.32	$\Gamma_{HCCC}(48) + \Gamma_{NCCH}(22)$
42	899	863			0.18	0.88	$\Gamma_{HCCC}(48) + \Gamma_{NCCH}(16)$
43	911	875	873w		4.42	1.89	$\nu_{CC}(14) + \delta_{CNC}(14) + \delta_{CCN}(10)$
44	942	905	904w		4.27	0.39	$\Gamma_{H8C4C3H7}(20) + \Gamma_{H10C6C5H9}(20)$
45	978	939			0.15	0.34	$\Gamma_{H23C19C16H20}(16) + \Gamma_{H35C30C28H31}(16)$
46	981	943			0.10	0.51	$\Gamma_{H23C19C16H20}(15) + \Gamma_{H35C30C28H31}(15)$
47	982	943			0.28	0.44	$\Gamma_{H8C4C3H7}(16) + \Gamma_{H9C5C4H8}(29) + \Gamma_{H10C6C5H9}(16)$
48	1003	964	961w		0.49	0.21	$\Gamma_{H13C12N11C1}(13) + \Gamma_{H26C25N24C2}(13)$
49	1004	964			0.26	0.61	$\Gamma_{HCNC}(18) + \Gamma_{HCCH}(20) + \Gamma_{CCCH}(18) + \Gamma_{CCCH}(18)$
50	1009	970			5.22	6.07	$\Gamma_{H22C17C15H18}(18) + \Gamma_{H36C32C29H33}(18)$
51	1010	970	1003w		4.94	11.29	$\Gamma_{HCCH}(18) + \Gamma_{HCNC}(10)$
52	1011	972	1008w	1006 ms	3.93	0.57	$\nu_{CC}(15) + \nu_{NC}(26)$
53	1014	974			7.10	4.43	$\nu_{NC}(17) + \Gamma_{HCCH}(10)$
54	1075	1032	1024 m		3.81	3.73	$\nu_{C4C3}(13) + \nu_{C5C4}(35) + \nu_{C6C5}(13) + \delta_{CCH}(20)$
55	1089	1046	1043 m		4.57	0.38	$\nu_{NC}(21) + \delta_{HCC}(30)$
56	1089	1046			3.48	0.70	$\nu_{N21C17}(7) + \nu_{N21C19}(4) + \nu_{N34C30}(4) + \nu_{N34C32}(7) + \delta_{HCC}(30)$
57	1111	1067			4.66	0.50	$\nu_{C19C16}(11) + \nu_{C30C28}(11)$
58	1112	1068			0.24	0.96	$\nu_{C19C16}(11) + \nu_{C30C28}(11)$
59	1129	1085	1094w		15.58	2.74	$\nu_{C4C3}(11) + \nu_{C6C5}(11) + \delta_{CCC}(14) + \delta_{CCH}(34)$
60	1188	1141	1137w	1148w	0.06	10.41	$\delta_{H8C4C3}(16) + \delta_{C5C4H8}(15) + \delta_{H9C5C4}(15) + \delta_{C6C5H9}(16)$
61	1212	1165	1156w		17.86	14.11	$\nu_{CC}(24) + \nu_{NC}(18) + \delta_{HCC}(18)$
62	1220	1172			35.92	87.72	$\nu_{CC}(36) + \nu_{NC}(18)$
63	1242	1193	1189 ms		0.77	1.36	$\nu_{NC}(20) + \delta_{CCH}(16) + \delta_{NCH}(24)$
64	1245	1196			8.27	2.45	$\nu_{NC}(26) + \delta_{NCH}(24) + \delta_{CCH}(14)$
65	1268	1219			0.76	6.64	$\nu_{C14C12}(10) + \nu_{C27C25}(10)$
66	1274	1224	1227 ms	1224w	0.00	0.40	$\nu_{NC}(18) + \nu_{CC}(18) + \delta_{HCN}(10)$
67	1299	1248			0.63	0.53	$\nu_{CC}(26) + \nu_{NC}(36) + \delta_{HCC}(12)$
68	1300	1249			8.98	5.66	$\nu_{N21C17}(10) + \nu_{N21C19}(13) + \nu_{N34C30}(13) + \nu_{N34C32}(10)$
69	1306	1255		1253 ms	6.06	6.31	$\nu_{NC}(22) + \delta_{CCH}(34)$
70	1334	1282	1283 ms		7.47	10.86	$\nu_{C2C1}(20) + \nu_{C3C2}(16) + \nu_{C5C4(10)} + \nu_{C6C1}(16)$
71	1356	1303		1297 ms	4.78	1.39	$\delta_{HCC}(60)$
72	1358	1305	1315 ms		12.50	2.74	$\delta_{CCH}(10) + \delta_{HCC}(31)$

(*continued on next page*)

Table 1 (*continued*)

Mode nos.	Calculated frequencies (cm^{-1})		Observed frequencies (cm^{-1})		Intensities		Vibrational assignments TED[d] (⩾10%)
	Unscaled	Scaled[a]	FT-IR	FT-Raman	I_{IR}[b]	I_{Raman}[c]	
73	1410	1354	1342w		8.74	0.91	$\delta_{H13C12N11}(16) + \delta_{H13C12C14}(12) + \delta_{H26C25N24}(16) + \delta_{H26C25C27}(12)$
74	1411	1355			4.92	0.14	$\delta_{H13C12N11}(18) + \delta_{H13C12C14}(13) + \delta_{H26C25N24}(18) + \delta_{H26C25C27}(13)$
75	1454	1397			8.02	1.37	$\nu_{CC}(24) + \delta_{NCH}(31)$
76	1454	1397			19.93	0.75	$\nu_{CC}(24) + \delta_{NCH}(30)$
77	1481	1423	1426s	1421w	5.34	4.46	$\delta_{H8C4C3}(10) + \delta_{C5C4H8}(15) + \delta_{H9C5C4}(15) + \delta_{C6C5H9}(10)$
78	1516	1457	1448s	1452s	12.08	28.32	$\nu_{C2C1}(13)$
79	1535	1475	1465w		1.28	2.07	$\nu_{NC}(14) + \delta_{NCH}(18) + \delta_{HCC}(24)$
80	1537	1477	1488w	1474s	2.71	0.26	$\delta_{HCC}(22) + \delta_{NCH}(18)$
81	1609	1546	1535w	1527 m	0.00	18.37	$\nu_{C15C14}(11) + \nu_{C16C14}(10) + \nu_{C29C27}(11)$
82	1609	1546			47.79	8.58	$\nu_{C15C14}(11) + \nu_{C16C14}(11) + \nu_{C28C27}(11) + \nu_{C29C27}(11)$
83	1619	1556			0.26	16.73	$\nu_{C2C1}(15) + \nu_{C5C4}(28)$
84	1631	1567	1576 ms	1571s	5.95	52.50	$\nu_{C3C2}(13) + \nu_{C4C3}(18) + \nu_{C6C1}(13) + \nu_{C6C5}(18)$
85	1649	1584			41.59	16.56	$\nu_{C17C15}(10) + \nu_{C32C29}(10)$
86	1649	1585	1590w	1591s	35.33	25.89	$\nu_{C17C15}(10) + \nu_{C32C29}(10)$
87	1705	1638	1638w		40.69	100.0	$\nu_{C12N11}(38) + \nu_{C25N24}(38)$
88	1707	1640	1639w		100.00	47.23	$\nu_{C12N11}(38) + \nu_{C25N24}(38)$
89	3024	2906			31.82	0.39	$\nu_{C12H13}(50) + \nu_{C25\ H26}(50)$
90	3025	2906			34.95	0.46	$\nu_{C12H13}(50) + \nu_{C25H26}(50)$
91	3165	3041	2985w		47.61	0.84	$\nu_{C19H23}(41) + \nu_{C30H35}(39)$
92	3165	3041			1.04	2.12	$\nu_{C19H23}(39) + \nu_{C30H35}(41)$
93	3171	3047			10.97	0.52	$\nu_{C17H22}(47) + \nu_{C32H36}(47)$
94	3171	3047	3042 ms		33.03	1.49	$\nu_{C17H22}(47) + \nu_{C32H36}(47)$
95	3185	3060			1.13	0.15	$\nu_{C3H7}(18) + \nu_{C4H8}(32) + \nu_{C5H9}(32) + \nu_{C6H10}(18)$
96	3192	3067			29.31	0.26	$\nu_{C3H7}(18) + \nu_{C6H10}(18) + \nu_{C16H20}(22) + \nu_{C28H31}(21)$
97	3192	3067			1.63	2.01	$\nu_{C16H20}(39) + \nu_{C28H31}(40)$
98	3193	3068			3.32	0.89	$\nu_{C3H7}(20) + \nu_{C6H10}(20) + \nu_{C16H20}(18) + \nu_{C28H31}(18)$
99	3201	3076			13.49	0.70	$\nu_{C3H7}(32) + \nu_{C4H8}(18) + \nu_{C5H9}(18) + \nu_{C6H10}(32)$
100	3212	3086	3085w		20.49	2.58	$\nu_{C3H7}(12) + \nu_{C4H8}(38) + \nu_{C5H9}(38) + \nu_{C6H10}(12)$
101	3226	3100	3165w		1.44	0.03	$\nu_{C15H18}(47) + \nu_{C29H33}(50)$
102	3226	3100			3.04	0.72	$\nu_{C15H18}(50) + \nu_{C29H33}(46)$

ν: Stretching, δ: in-plane-bending, Γ: out-of-plane bending, vw: very week, w: week, m: medium, s: strong, vs: very strong.

[a] Scaling factor: 0.9608 [28].

[b] Relative IR absorption intensities normalized with highest peak absorption equal to 100.

[c] Relative Raman intensities calculated by Eq. (2.1) and normalized to 100.

[d] Total energy distribution calculated at B3LYP/6-31G(d,p) level.

slightly longer than the literature values because the molecular states were different during the experimental and theoretical process. The isolated molecule is considered as in gas phase during theoretical calculation, while many packing molecules were treated as in the condensed phase during the experimental measurements.

In this study, the packing of the two pyridine rings through N=C—H linkage on the benzene ring (at C1 and C2) cause some changes in the C—C bond length. They vary by 0.024 Å in the most extreme case within the same method of calculations. The benzene ring is little distorted in which the C1—C2 (1.419 Å), and C1—C6/C2—C3 (1.402 Å) bond lengths are longer than the bonds C3—C4, C4—C5 and C5—C6 (~1.395 Å). The increasing of bond lengths at C1—C2, C1—N11 and C2—N24 bonds is due to slightly irregular hexagonal structure of the angles C2—C1—C6/C1—C2—C3 and C2—C3—C4/C1—C6—C5 are 119.06° and 121.07° respectively. The C—H bond lengths are found to be 1.086 Å in benzene ring, while C12—H13/C25—H26 bond length is about 1.100 Å. The lengths bond and bond angles of both pyridine rings are identical.

4.3. Vibrational assignments

The NBPMB is a non-planar molecule and possesses C_1 point group symmetry. The molecule has 36 atoms and hence 102 normal modes of vibrations were possible, which were active in both IR absorption and Raman scattering. The harmonic vibrational frequencies were calculated at B3LYP level with 6-31G(d,p) basis set and which are summarized in Table 1. In the last column of Table 1, a detailed description of the normal modes based on the TED is given. Furthermore, none of the predicted vibrational spectra have any imaginary wavenumbers, implying that the optimized geometry is located at the local lowest point on the potential energy surface. Comparison of the frequencies calculated at B3LYP with experimental assignments reveal the overestimation of the calculated vibrational modes due to the neglect of anharmonicity in the real system. We know that the *ab initio* HF and DFT potentials systematically overestimate the vibrational wavenumbers. These discrepancies are corrected by computing anharmonic corrections explicitly, by introducing a scaled field [26] or directly scaling the calculated wavenumbers with the proper factor [27]. The scale factor 0.9608 [28] was used to bring the computed wavenumbers close to the recorded frequencies. The combined experimental and theoretical spectra are shown in Fig. 2 (FT-IR) and 3 (FT-Raman) (see Fig. 3).

4.3.1. C—H vibrations

The presence of one or more aromatic rings in a structure is normally readily determined from the C—H and C=C—C ring related vibrations [29]. The C—H stretching vibration occurs above 3000 cm^{-1} and is typically exhibited as multiplicity of the weak to moderate bands, compared with the aliphatic C—H stretch [30]. The heteroaromatic structure has shown the presence of C—H stretching vibration in the region of 3100–3000 cm^{-1} which was the characteristic region for the ready identification of C—H stretching vibrations [31].

In the present study, the harmonic C—H stretching vibrations (benzene) are assigned in the range 3086–3060 cm^{-1} (mode nos: 100, 99, 98, 95), while the observed FT-IR band is at 3085 cm^{-1}. Similarly the observed bands (FT-IR) 3165, 3042 cm^{-1} and calculated frequencies lies in the range 3100–3041 cm^{-1} (mode nos:

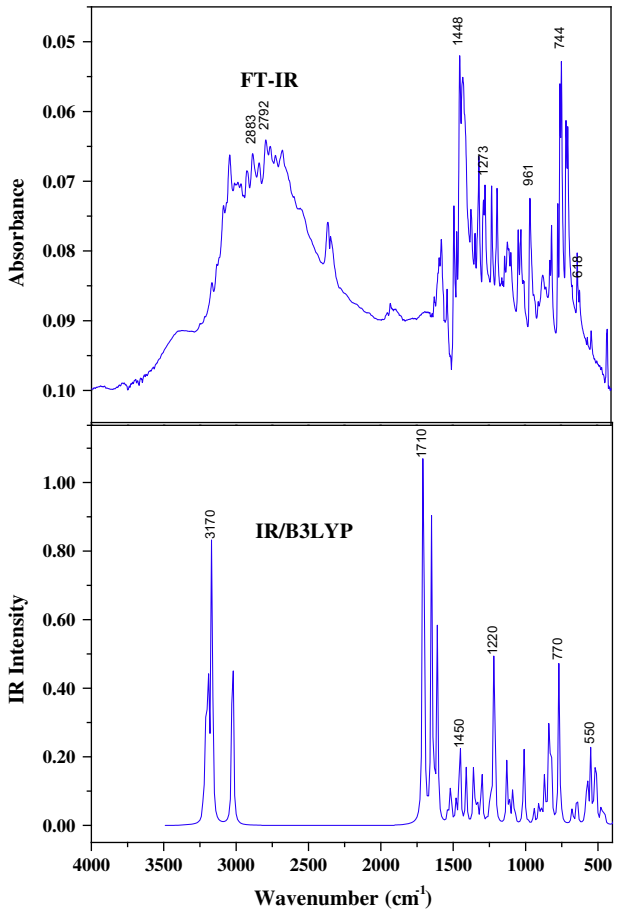

Fig. 2. The combined FT-IR and simulated IR spectra of NBPMB.

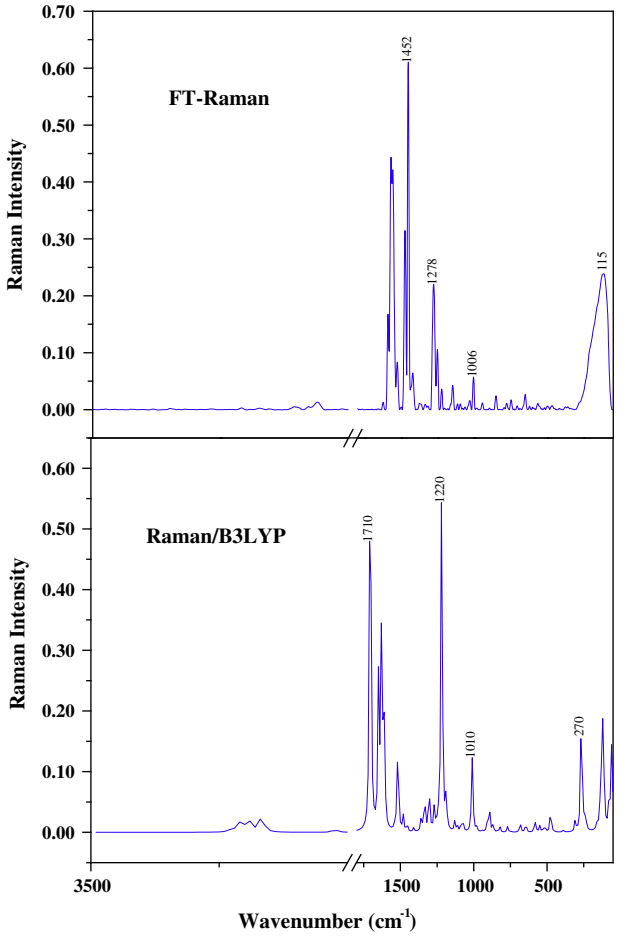

Fig. 3. The combined FT-Raman and simulated Raman spectra of NBPMB.

102, 101, 97, 96, 94–91) are assigned to νC—H stretching for pyridine rings. These assignments are shown as good correlation with literature values [29], and also within the expected range. As it is evident from the TED column, the mode nos: 102–91 is pure stretching modes (<80%). The mode nos: 90 and 89 are assigned to νC—H in methylene diamine linkage (C12—H3, C25—H26) with 100% TED. All the aromatic C—H stretching bands are found to be weak and this is due to the decrease of the dipole moment caused by the reduction of negative charge on the carbon atom.

In aromatic compounds, the C—H in-plane bending vibrations appear in the range 1000–1300 cm^{-1} and the C—H out-of-plane bending vibrations appear in the range 750–1000 cm^{-1} [32]. The bands are sharp but weak to medium intensity. The weak and medium intensity bands at 1137, 1156 and 1227, 1426 cm^{-1} (strong) in FT-IR spectrum are due to in-plane C—H bending of benzene ring. In-plane bending of C—H bonds is recorded at 1148, 1224 and 1421 cm^{-1}. These recorded values are in parallel with the calculated wavenumbers at 1141, 1165, 1224 and 1423 cm^{-1} (mode nos: 60, 61, 66, and 77). Most of the vibrations were not pure but contains a significant contribution from other modes. These assignments were supported by literature values [33]. The FT-IR bands at 1043, 1189, 1315 cm^{-1} and the FT-Raman bands 1253, 1297 cm^{-1} are assigned to C—H in-plane bending vibrations of pyridine rings in NBPMB. These assignments are comparable with harmonic wavenumbers in range 1046–1305 cm^{-1} (mode nos: 55, 56, 63, 64, 67, 69, 71, 72) and also find support from literature [34,35]. The mode numbers 73, 74 are assigned to δ_{C-H} (C_{12}—H_{13}, C_{25}—H_{26}) modes. These vibrations show considerable TED values.

Generally, the C—H out-of-plane deformations with the highest wavenumbers have weaker intensity than those absorbing at lower wavenumbers. In this study, the Γ_{C-H} modes are assigned at 743, 823 and 904 cm^{-1} in FT-IR spectrum. These assignments are in agreement with literature [33–35] and also within the characteristic region. The mode numbers 48, 49 are belongs to Γ_{C-H} (C_{12}—H_{13}/C_{25}—H_{26}) modes.

4.3.2. C—N vibrations

The C=N stretching appears in the region 1670–1600 cm^{-1} [36]. In the present study the band due to C=N stretching vibrations are recorded at 1639 and 1638 cm^{-1} ($\nu_{C12-N11}$, $\nu_{C25-N24}$) in FT-IR and their corresponding calculated values are about 1640 and 1638 cm^{-1} (mode nos: 88, 87). The TED of this mode was shown in such a way that they were moderately pure stretching mode (78%). Karabacak et al. [37] observed the C—N stretching vibrations at 1213 and 1189 cm^{-1} (harmonic) for *N*-(2-methylphenyl) methane sulfonamide. In the present study, the observed FT-IR band 1189 cm^{-1} (medium) is attributed to C—N stretching. The theoretically calculated values of C—N (C1—N11; C2—N24) stretching vibrations are 1196, 1193 cm^{-1} (mode nos: 64, 63), in which mode number 63 is in line with experimental data. In 1,3-bis (4-pyridyl) propane [34], the C—N stretching bands were found to be 1038 and 1252 cm^{-1}.

Based on the these factors, in the present work, the observed frequency 1043 cm^{-1}/FT-IR and the predicted frequencies 1046, 1248, 1249 cm^{-1} (mode nos: 55, 56, 67, 68) are due to C—N stretching in pyridine rings. These assignments are further supported from TED values. Erdoğdu et al. [34] observed δ_{NCH} and δ_{CNC} vibration in the region 1215–1509 cm^{-1} and at 826 cm^{-1} respectively for 1,3 bis (4-pyridyl) propane. The DFT

calculation gives the wavenumbers 1397, 1397, 1475, 1477 (mode nos: 75, 76, 79, 80) are assigned to be N—C—H in-plane bending vibration (pyridine ring). While $\delta_{N11=C12-H13}/\delta_{N24=C25-H26}$ is assigned to harmonic wavenumber 1354/1355 cm^{-1} (mode nos: 73, 74) respectively. The harmonic frequencies at 620, 650 cm^{-1} (mode nos: 27, 28) are attributed to δ_{C-N-C} mode in both pyridine rings. These assignments are supported by observed bands 1465, 1488, 1342, 618 in FT-IR and 1474, 652 cm^{-1} in FT-Raman spectra. The harmonic frequencies of mode numbers 48, 49 (964, 964 cm^{-1}) are assigned to $\Gamma_{N11=C12-H13}/\Gamma_{N24=C25-H26}$ vibrations, whereas the frequency 961 cm^{-1} in FT-IR spectrum supports the mode numbers 48 and 49.

4.3.3. C—C vibrations

In general, the bands around 1600 and 1400 cm^{-1} in benzene are assigned to skeletal C—C stretching modes [38]. In this work, the middle to strong bands are observed at 1576, 1448, 1283, 1094 cm^{-1} in FT-IR and strong bands observed at 1571, 1452 cm^{-1} in FT-Raman are assigned to aromatic C—C stretching vibrations (benzene ring), which are good agreement with theoretically calculated value at 1567–1085 cm^{-1} (mode nos: 84, 83, 78, 70, 62, 59). These assignments find support from the work of Fereyduni et al. [29] and are within the frequency intervals given by Varsanyi [38]. Similarly the frequencies observed in FT-IR spectrum at 1590, 1535, 1008, 873 cm^{-1} are assigned to C—C stretching vibrations for pyridine. The corresponding vibrations appear in the FT-Raman spectrum at 1591, 1527 and 1006 cm^{-1}. The computed values in the range 1585–875 cm^{-1} (mode nos: 86, 85, 82, 81, 76, 75, 52, 43) shows good coherence with experimental data and also in line with literature value [39]. These assignments are also supported by TED values.

The ring (benzene) in-plane deformation vibrations are ascribed to the FT-IR band at 1094, 618 cm^{-1} and harmonic bands at 1085, 835 and 620 cm^{-1} (mode nos: 59, 39, 27). The C—C—C out-of-plane deformations (benzene) are found at 712, 564 cm^{-1} FT-IR bands and the harmonic bands at 735, 716, 560 cm^{-1} (mode nos: 33, 31, 25). Similarly the C—C—C in-plane-bending vibrations (pyridine) are attributed to the harmonic bands in the range 657–437 cm^{-1} (mode nos: 30, 29, 21, 19) and the FT-IR bands at 670, 499, 426 cm^{-1}. The out-of-plane vibrations due to C—C—C (pyridine) are characterized by the harmonic bands at 725, 716, 375 and 248 cm^{-1} (mode nos: 32, 31, 18, 17, and 12). These assignments are supported by Sundaraganesan et al. [39], Erdoğdu et al. [34] and Wang et al. [40] for pyridine and benzene rings.

4.4. Hyperpolarizability calculations

The first order hyperpolarizabilities (β_0, α_0 and $\Delta\alpha$) of NBPMB is calculated using B3LYP/6-31G(d,p) basis set, based on the finite-field approach. In the presence of an applied electric field, the energy of a system is a function of the electric field. First hyperpolarizability is a third rank tensor that can be described by a $3 \times 3 \times 3$ matrix. The 27 components of the 3D matrix can be reduced to 10 components due to Kleinman symmetry [41]. It can be given in the lower tetrahedral format. It is obvious that the lower part of the $3 \times 3 \times 3$ matrix is a tetrahedral. The components of β are defined as the coefficients in the Taylor series expansion of the energy in the external electric field. When the external electric field is weak and homogeneous, this expansion becomes:

$$E = E^0 - \mu_\alpha F_\alpha - 1/2\alpha_{\alpha\beta}F_\alpha F_\beta - 1/6\beta_{\alpha\beta\gamma}F_\alpha F_\beta F_\gamma \quad (2)$$

where E^0 is the energy of the unperturbed molecules, F_α is the field at the origin, and μ_α, $\alpha_{\alpha\beta}$, $\beta_{\alpha\beta\gamma}$ are the components of the dipole moment, polarizability and the first order hyperpolarizabilities respectively. The total static dipole moment μ, the mean polarizability α_0, the anisotropy of polarizability $\Delta\alpha$ and the mean first hyperpolarizability β_0, using the x, y, z components are defined as

$$\mu = (\mu_x^2 + \mu_y^2 + \mu_z^2)^{1/2} \quad (3)$$

$$\alpha_0 = \frac{\alpha_{xx} + \alpha_{yy} + \alpha_{zz}}{3} \quad (4)$$

$$\Delta\alpha = 2^{-1/2}[(\alpha_{xx} - \alpha_{yy})^2 + (\alpha_{yy} - \alpha_{zz})^2 + (\alpha_{zz} - \alpha_{xx})^2 + 6(\alpha_{xy}^2 + \alpha_{yz}^2 + \alpha_{xz}^2)]^{1/2} \quad (5)$$

$$\beta_0 = (\beta_x^2 + \beta_y^2 + \beta_z^2)^{1/2} \quad (6)$$

Many organic molecules, containing conjugated π electrons were characterized by large values of molecular first order hyper polarizabilities and analyzed by means of vibrational spectroscopy [42–45]. The intra molecular charge transfer from the donor to acceptor group through a single-double bond conjugated path can induce large variations on both the molecular dipole moment and the molecular polarizability making IR and Raman activity strong at the same time [46].

The total molecular dipole moment (μ) and mean first order hyperpolarizability (β_0) are given as 1.714 Debye and 1.117×10^{-30} esu, respectively. The total dipole moment of the title compound is approximately higher and the first order hyperpolarizability (β_0) of the title molecule is three times greater than that of urea, hence this molecule has considerable NLO activity. The computation of the molecular polarizability of NBPMB is shown in Table 2.

4.5. NBO analysis

The hyperconjugation may be given as stabilizing effect that arises from an overlap between an occupied orbital with another neighboring electron deficient orbital, when these orbitals are properly orientated. This non-covalent bonding (antibonding)

Table 2
The molecular dipole moment (μ), polarizability (α) and hyperpolarizability (β_0) values of NBPMB.

Parameters	B3LYP/6-31G(d,p)
Dipole moment (μ)	
μ_x	0.0001
μ_y	1.7143
μ_z	−0.0001
μ	1.7143 Debye
Polarizability (α)	
α_{xx}	311.07
α_{xy}	0.00
α_{yy}	299.77
α_{xz}	32.03
α_{yz}	−0.01
α_{zz}	109.67
α	6.47×10^{-30} esu
Hyperpolarizability (β_0)	
β_{xxx}	−0.13
β_{xxy}	−837.08
β_{xyy}	0.07
β_{yyy}	−473.04
β_{xxz}	0.02
β_{xyz}	−53.46
β_{yyz}	0.02
β_{xzz}	0.00
β_{yzz}	17.48
β_{zzz}	0.00
β_0	1.1167×10^{-30} esu

Standard value for urea μ = 1.3732 Debye, $\beta_0 = 0.3728 \times 10^{-30}$ esu.

Table 3
The NBO results showing the following of Lewis and non-Lewis for orbitals for NBPMB.

Bond (A—B)	ED/e	ED_A%	ED_B%	NBO	s%	p%
C1—C2	1.96151	50.00	50.00	$0.7071sp^{1.85}$C	35.03	64.93
	−0.70773			$+0.7071sp^{1.85}$C	35.03	64.93
C1—C6	1.97074	51.01	48.99	$0.7142sp^{1.71}$ C	36.95	63.02
	−0.71752			$-0.6999sp^{1.85}$ C	35.11	64.84
C1—C6(2)	1.6643	49.49	50.51	$0.7035sp^{1.00}$ C	0.01	99.96
	−0.26823			$+0.7107sp^{99.99}$ C	0.02	99.93
C1—N11	1.97716	41.09	58.91	$0.6410sp^{2.58}$ C	27.88	72.02
	−0.77555			$-0.7675sp^{2.11}$N	32.14	67.79
C2—C3	1.97075	51.01	48.99	$0.7142sp^{1.71}$ C	36.95	63.02
	−0.71752			$+0.6999sp^{1.85}$ C	35.11	64.84
C2—C3(2)	1.66429	49.49	50.51	$0.7035sp^{1.00}$ C	0.01	99.96
	−0.26823			$-0.7107sp^{99.99}$ C	0.02	99.93
C3—H7	1.97788	60.48	39.52	$0.7777sp^{2.50}$ C	28.52	71.43
	−0.53209			$+0.6287sp^{0.00}$H	99.96	0.04
C4—H8	1.97941	60.36	39.64	$0.7769sp^{2.49}$ C	28.64	71.32
	−0.52857			$-0.6296sp^{0.00}$H	99.95	0.05
C29—H33	1.97777	61.59	38.41	$0.7848sp^{2.33}$ C	29.99	69.97
	−0.53174			$-0.6197sp^{0.00}$H	99.95	0.05
C17—H22	1.98171	59.74	40.26	$0.7729sp^{2.42}$ C	29.23	70.72
	−0.53016			$+0.6345sp^{0.00}$H	99.95	0.05
C32—H36	1.98171	59.74	40.26	$0.77729sp^{2.42}$ C	29.23	70.72
	1.98171			$-0.6345sp^{0.00}$H	99.95	0.05
C19—H23	1.98185	59.69	40.31	$0.7726sp^{2.42}$ C	29.25	70.70
	−0.53312			$+0.6349sp^{0.00}$H	99.95	0.05
C30—H35	1.98185	59.69	40.31	$0.7726sp^{2.42}$ C	29.5	70.70
	−0.53312			$-0.6349sp^{0.00}$H	99.95	0.05
LPN11	1.87249			$sp^{2.65}$	27.15	72.78
	−0.35637					
LPN21	1.91459			$sp^{2.65}$	27.35	72.57
	−0.34135					
LPN24	1.87252			$sp^{2.68}$	27.15	72.78
	−0.35638					
LPN34	1.91459			$sp^{2.65}$	27.35	72.57
	−0.34135					

s, p – Are orbitals, A,B – denotes atoms, ED – electron density.

interaction can be quantitatively described in terms of the NBO analysis, which is expressed by means of the second-order perturbation interaction energy ($E^{(2)}$) [47–50]. This energy represents the estimate of the off-diagonal NBO Fock matrix elements. It can be deduced from the second-order perturbation approach [51]

$$E^{(2)} = \Delta E_{ij} = q_i \frac{F(i,j)^2}{\varepsilon_j - \varepsilon_i} \quad (7)$$

where q_i is the donor orbital occupancy, ε_i and ε_j are diagonal elements (orbital energies) and $F(i,j)$ is the off diagonal NBO Fock matrix elements. NBO analysis of NBPMB has been performed, in order to explain the intra-molecular charge transfer and delocalization of π-electrons. The intra-molecular hyperconjugative interaction is due to the overlap between π(C—C) and π*(C—C) the orbitals, which results in intra molecular charge transfer, appeared in the molecular system [46].

In the present study, the electron densities of the σ bonds are higher than π bonds. The lowering of the electron densities is due to transfer of lone electron pair from donor to acceptor (anti bonding) orbital. This is the evident from the Table S3 that the electron densities of $\sigma C_1—C_2$, $C_1—C_6$, $C_2—C_3$, $C_4—C_5$, and $C_5—C_6$ are about 1.962, 1.971, 1.971, 1.978 and 1.976 e respectively. Their corresponding anti-bonding acceptor orbital is having weak electron densities with lesser hyperconjugative energy ($E^{(2)}$). On the other hand, the occupancy of $\pi C_1—C_6$, $C_2—C_3$ and $C_4—C_5$ are decreased by increasing the electron densities of their corresponding anti-bonding acceptor orbitals with maximum $E^{(2)}$ energy. The donor and acceptor interactions of $\pi(C_1—C_6) \rightarrow \pi^*(C_2—C_3, C_4—C_5, N_{11}—C_{12})$; $\pi(C_2—C_3) \rightarrow \pi^*(C_1—C_6, C_4—C_5, N_{24}—C_{25})$ and $\pi(C_4—C_5) \rightarrow (C_1—C_6, C_2—C_3)$ revealed the maximum hyperconjugative interaction in benzene ring. It has been observed in both pyridine rings.

It is evident from the Table S3, the n—π* transition for N_{11}, N_{21}, N_{24} and N_{34} have maximum $E^{(2)}$ energy. In this study, the BD* to BD* (anti-bond π*—π*) interactions ($BD^*C_{19}—N_{27} \rightarrow C_{14}—C_{16}$, $C_{15}—C_{17}$) and ($BD^* C_{30}—N_{34} \rightarrow C_{27}—C_{28}$, $C_{29}—C_{32}$) reveal the maximum $E^{(2)}$ energy 1135.29, 616.86 and 1135.08, 616.81 kJ/mol respectively. From the Table 3, the electron density of $\sigma C_1—C_6$ is 1.970 e and the electron density value of C_1 and C_6 are 36.95 (s-orbital), 63.02 (p-orbital) and 35.11 (s-orbital), 64.84% (p-orbital) respectively. In the $\pi C_1—C_6$ bond, the p-character for C_1 and C_6 are 99.9% on comparing with s-character. This clearly shows that the higher values of p-character causes the interaction and hence the charge transfer is more in the acceptor orbital with decreasing occupancy in $C_1—C_6$ (1.664e).

4.6. HOMO–LUMO analysis

Stability of the molecule depends on the band gap between the highest filled and lowest unfilled orbitals. The lower band gap increases the reactivity of the molecule while the higher band gap decreases the reactivity. The HOMO and LUMO energy calculated by B3LYP/6-31G(d,p) method has been shown in Table 4. In the present study, band gap between HOMO and LUMO is calculated about -3.9568 eV. The HOMO part is located over the benzene ring and diamine bond (C—N=C). The LUMO is located over the each atom of the molecule. On the basis of fully optimized ground-state structure, TD-DFT/B3LYP/6-31G(d,p) calculation have been used to determine the low-lying excited states of NBPMB. The calculated results involving the vertical excitation energies, oscillator strength (f) and wavelength are carried out and compared with measured experimental wavelength. For NBPMB, the TD-DFT

Table 4
The electronic transition of NBPMB.

Calculated at B3LYP/6-31G(d,p)	Oscillator strength and excitation energies	Experimental band gap (nm)	Calculated band gap (eV/nm)
Excited state 1			
	Singlet-A/f = 0.0965		382.21 nm/3.2439 eV
75 − >76 (HOMO–LUMO)	0.66888		−3.9568
Excited state 2			
	Singlet-A/f = 0.0744	336.47	336.18 nm/3.6880 eV
75 − >77 ($HOMO–LUMO_{+1}$)	0.66932		−4.3584
Excited state 3			
	Singlet-A/f = 0.0123	306.43	306.15 nm/4.0498 eV
72 − >76($HOMO_{-3}$–LUMO)	0.45773		−4.8749
73 − >77($HOMO_{-2}$–$LUMO_{+1}$)	−0.28627		−5.2722
74 − >76($HOMO_{-1}$–LUMO)	−0.41308		−4.6763

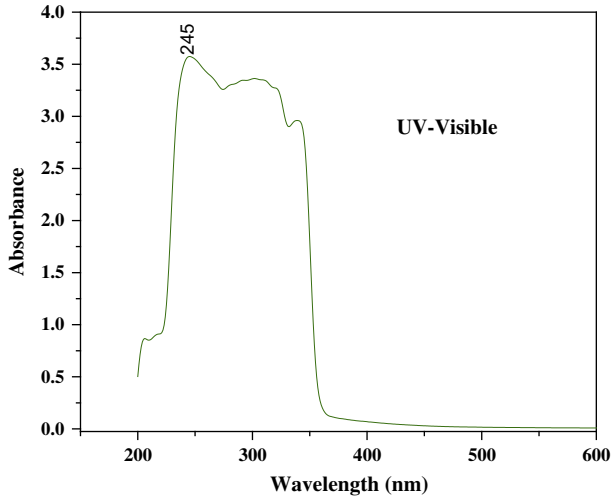

Fig. 4. The experimental UV–Vis spectrum of NBPMB.

calculations predict the wavelengths 382, 336 and 306 nm are corresponding to transitions HOMO–LUMO, HOMO–$LUMO_{+1}$ and $HOMO_{-3}$–LUMO respectively. The observed band gaps 336.47 and 306.43 nm are in agreement with the calculated values 381.21 (E_1), 336.18 (E_2) and 306.15 nm (E_3). The observed UV–Vis spectra and HOMO and LUMO plots are shown in Fig. 4 and Figure S2 (Supporting information) respectively.

5. Conclusions

The observed FT-IR and FT-Raman spectral values were agreed well with the calculated wavenumbers. For the prediction of accurate vibrational assignments TED were calculated using SQM method. The conformer one is more stable and hence the calculated bond length and bond angles were correlated well with the experimental values. The NBO analysis reveals the occurrence of hyperconjugative interaction and charge delocalization around the bonds. It also reflects the charge transfer mainly due to C_{19}—N_{21} and C_{30}—N_{34} groups. The presence of C═N fused with two pyridine rings, increases the molecular hyperpolarizability of title compound about 1.116×10^{-30} esu, which is three times higher than that of urea. The HOMO–LUMO energy gap indicates the stability and reactivity of the title compound. Moreover, HOMO-1, -2 are mainly located over N═C group.

Appendix A. Supplementary material

Supplementary data associated with this article can be found, in the online version, at http://dx.doi.org/10.1016/j.molstruc.2013.03.034.

References

[1] E. Keskioglu, A. BalabanGunduzalp, F. Hamurw, Spectrochim. Acta A 70 (2008) 634–640.
[2] M.S. Karthikeyan, D.J. Prasad, B. Poojary, Bioorg. Med. Chem. 14 (2006) 7482.
[3] K. Singh, M.S. Barwa, P. Tyaji, Eur. J. Med. Chem. 41 (2006) 1.
[4] S.K. Sridhar, M. Sarvan, A. Ramesh, Eur. J. Med. Chem. 36 (2001) 615.
[5] J.N. Pandeya, Eur. J. Pharmacol. 9 (1999) 25.
[6] R. Mladenora, M. Ignatova, N. Manolova, J. Petrova, Eur. Polym. J. 38 (2002) 989.
[7] O.M. Walsh, M.J. Meegan, R.M. Prendergast, A.T. Nakib, Eur. J. Med. Chem. 31 (1996) 989.
[8] T.D. Thangadurai, M. Gowri, K. Natarajan, Synth. React. Inorg. Met-org. Chem. 32 (2002) 329.
[9] H.D. Revanasiddappa, K. Shiva Prasad, L. Shiva Kumar, I. J. C. R. 2 (2010) 1344–1349.
[10] G. Hoffle, W. Steglich, H. Vorbruggen, Chem. Int. Ed. 17 (1978) 569.
[11] R.N. Medhi, R. Barman, K.C. Medhi, S.S. Jois, Spectrochim. Acta A 56 (2000) 1523.
[12] A. Topacli, S. Bayari, Spectrochim. Acta 57 (2001) 1385.
[13] N. Sundaraganesan, H. Saleem, S. Mohan, Spectrochim. Acta A 59 (2003) 1113–1118.
[14] V. Krishnakumar, S. Muthunatesan, Spectrochim. Acta A 65 (2006) 818–825.
[15] W. Koch, M.C. Holthausen, A Chemists Guide to Density Functional Theory, Second Ed., Wiley-VCH VerlagGmbh, Weinheim, 2001.
[16] A.D. Becke, J. Chem. Phys. 98 (1993) 5648–5652.
[17] C. Lee, W. Yang, R.G. Parr, Phys. Rev. B37 (1988) 785–789.
[18] Spartan 08, Wavefunction Inc., Irvine, CA 92612, USA, 2008.
[19] M.J. Frisch, G.W. Trucks, H.B. Schlegel, G.E. Scuseria, M.A. Robb, J.R. Cheeseman, J.A. Montgomery, Jr., T. Vreven, K.N. Kudin, J.C. Burant, J.M. Millam, S.S. Iyengar, J. Tomasi, V. Barone, B. Mennucci, M. Cossi, G. Scalmani, N. Rega, G.A. Petersson, H. Nakatsuji, M. Hada, M. Ehara, K. Toyota, R. Fukuda, J. Hasegawa, M. Ishida, T. Nakajima, Y. Honda, O. Kitao, H. Nakai, M. Klene, X. Li, Knox, H.P. Hratchian, J.B. Cross, C. Adamo, J. Jaramillo, R. Gomperts, R.E. Stratmann, O. Yazyev, A.J. Austin, R. Cammi, C. Pomelli, J.W. Ochterski, P.Y. Ayala, K. Morokuma, G.A. Voth, P. Salvador, J.J. Dannenberg, V.G. Zakrzewski, S. Dapprich, A.D. Daniels, M.C. Strain, O. Farkas, D.K. Malick, A.D. Rabuck, K. Raghavachari, J.B. Foresman, J.V. Ortiz, Q. Cui, A.G. Baboul, S. Clifford, J. Cioslowski, B.B. Stefanov, G. Liu, A. Liashenko, P. Piskorz, I. Komaromi, R.L. Martin, D.J. Fox, T. Keith, M.A. Al-Laham, C.Y. Peng, A. Nanayakkara, M. Challacombe, P.M.W. Gill, B. Johnson, W. Chen, M.W. Wong, C. Gonzalez, J.A. Pople, Gaussian 03, Revision C.02, Gaussian, Inc., Wallingford, CT, 2004.
[20] H.B. Schlegel, J. Comput. Chem. 3 (1982) 214–218.
[21] G. Rauhut, P. Pulay, J. Phys. Chem. 99 (1995) 3093–3100.
[22] D. Michalska, Raint Program, Wroclaw University of Technology, 2003.
[23] D. Michalska, R. Wysokinski, Chem. Phys. Lett. 403 (2005) 211–217.
[24] I. Sheikhshoaie, V. Saheb, Spectrochim. Acta A 77 (2010) 1069–1076.
[25] R.S. Vadavi, R.V. Shenoy, D.S. Badiger, K.B. Gudasi, L.G. Devi, M. Nethaji, Spectrochim. Acta A 79 (2011) 348–355.
[26] P. Pulay, G. Fogarasi, G. Pongor, J.E. Boggs, V. Vargha, J. Am. Chem. Soc. 105 (1983) 7037.
[27] A.P. Scott, L. Random, J. Phys. Chem. 100 (1996) 16502.
[28] M.A. Palafox, Int. J. Quant. Chem. 77 (2000) 661–684.
[29] E. Fereyduni, E. Vessally, E. Yaaghubi, N. Sundaraganesan, Spectrochim. Acta A 81 (2011) 64–71.
[30] J. Coates, R.A. Meyers, Interpretation of Infrared Spectra: A Practical Approach, John Wiley and sons Ltd, Chichester, 2000.
[31] M. Silverstein, C.G. Basseler, C. Morill, Spectrometric Identification of Organic Compounds, Wiley, New York, 1981.
[32] G. Varsanyi, Assignments of Vibrational Spectra of 700 Benzene Derivatives, Wiley, New York, 1974.
[33] H.T. Varghese, C.Y. Paniker, V.S. Madhavan, S. Mathew, J. Vinsova, C.V. Alsenoy, J. Raman Spectrosc. 40 (2009) 1211–1223.
[34] Y. Erdoğdu, M.T. Güllüoğlu, M. Kurt, Spectrochim. Acta A 71 (2008) 377–387.
[35] N. Sundaraganesan, H. Umamaheswari, J.B. Dominic, C. Meganathan, M. Ramalingam, J. Mol. Struct. (Theochem) 850 (2008) 84.
[36] G. Socrates, Infrared Characteristic Group frequencies, John Wiley and Sons, Ltd., New York, 1980.
[37] M. Karabacak, M. Cinar, M. Kurt, J. Mol. Struct. 968 (2010) 108–114.
[38] G. Varsanyi, Vibrational Spectra of Benzene Derivatives, Academic Press, New York, 1969.
[39] N. Sundaraganesan, S. Ilakiyamani, B.D. Joushua, Spectrochim. Acta 67 A (2007) 287–297.
[40] Y. Wang, Z. Yu, Y. Sun, Y. Wang, L. Lu, Spectrochim. Acta A 79 (2011) 1475–1482.
[41] N.B. Colthup, L.H. Daly, S.E. Wiberly, Introduction to Infrared and Raman Spectroscopy, Academic Press, New York, 1990.
[42] C. Castiglioni, M. Del zoppo, P. Zuliani, G. Zerbi, Synth. Met. 74 (1995) 171–177.
[43] P. Zuliani, M. Del zoppo, C. Castiglioni, G. Zerbi, S.R. Marder, J.W. Perry, Chem. Phys. 103 (1995) 9935.
[44] M. Del zoppo, C. Castiglioni, G. Zerbi, Non-Linear Opt. 9 (1995) 73.
[45] M. Del zoppo, C. Castiglioni, P. Zuliani, A. Razelli, G. Zerbi, M. Blanchard-Desce, J. Appl. Polym. Sci. 70 (1998) 73.
[46] C. Ravikumar, I. Huber Joe, V.S. Jayakumar, Chem. Phys. Lett. 460 (2008) 552–558.
[47] A.E. Reed, F. Weinhold, J. Chem. Phys. 78 (1983) 4066–4073.
[48] A.E. Reed, F. Weinhold, J. Chem. Phys. 83 (1985) 1736–1740.
[49] A.E. Reed, R.B. Weinstock, F. Weinhold, J. Chem. Phys. 83 (1985) 735–746.
[50] J.P. Foster, F. Wienhold, J. Am. Chem. Soc. 102 (1980) 7211–7218.
[51] J. Chocholousova, V. Vladimir Spirko, P. Hobza, Phys. Chem. Chem. Phys. 6 (2004) 37–41.